Phase structure of a chiral model with dilatons in hot and dense matter

Chihiro Sasaki[1] and Igor Mishustin[1,2]
[1]*Frankfurt Institute for Advanced Studies, DE-60438 Frankfurt am Main, Germany*
[2]*Kurchatov Institute, Russian Research Center, Moscow RU-123182, Russia*
(Received 16 October 2011; revised manuscript received 2 February 2012; published 21 February 2012)

We explore the phase structure of a chiral model of constituent quarks and gluons implementing scale symmetry breaking at finite temperature and chemical potential. In this model the chiral dynamics is intimately linked to the trace anomaly saturated by a dilaton field. The thermodynamics is governed by two condensates, thermal expectation values of σ and dilaton fields, which are the order parameters responsible for the phase transitions associated with the chiral and scale symmetries. Within the mean-field approximation, we find that with increasing temperature, a system experiences a chiral phase transition, and then a first-order phase transition of partial scale symmetry restoration characterized by a melting gluon condensate takes place at a higher temperature. There exists a region at finite chemical potential where the scale symmetry remains dynamically broken while the chiral symmetry is restored. We also give a brief discussion on the σ-meson mass constrained from lattice QCD.

DOI: 10.1103/PhysRevC.85.025202 PACS number(s): 12.39.Fe, 12.39.Mk, 12.38.Mh, 21.65.−f

I. INTRODUCTION

Effective theories of strongly interacting matter are expected to capture nonperturbative aspects of QCD in the low-energy domain. They are constructed based on global symmetries of QCD Lagrangian and their breaking patterns. In the limit of massless quarks the Lagrangian possesses the chiral symmetry and scale invariance, both of which are dynamically broken in the physical vacuum due to the strong interaction. The QCD trace anomaly signals the emergence of a scale at the quantum level from the theory without any dimension-full parameters [1]. Thus spontaneous chiral symmetry breaking, which gives rise to a nucleon mass, and the trace anomaly are closely linked to each other [2], and dynamical scales in hadronic systems are considered to originate from them. How they behave under extreme conditions such as high temperature and density is one of the main issues in QCD [3].

The trace anomaly has been implemented in a chiral Lagrangian by introducing a dilaton (or glueball) field representing the gluon condensate $\langle G_{\mu\nu}G^{\mu\nu}\rangle$ [4]. Thermodynamics of the dilatons at finite temperature and density has also been explored and the deconfinement phase transition was studied [5]. Incorporating the QCD scaling properties into a nonlinear chiral Lagrangian, the in-medium scaling associated with chiral symmetry restoration, i.e., Brown-Rho (BR) scaling [6], was introduced, and some related works have been carried out [7,8]. Besides, along with the lattice QCD computations, pure gluon dynamics at finite temperature has been formulated in several approaches [9–13].

In this paper we introduce a model of constituent quarks and gluons implementing chiral and scale invariance in such a way that the model mimics the nonperturbative nature of QCD in low energies. We will explore the thermodynamics and constrain the σ-meson mass utilizing the QCD trace anomaly extracted from lattice QCD [12]. Imposing field theoretical requirements on the anomaly matching, we will give a suggestive phase diagram of QCD.

II. TOY MODEL

In this section we briefly introduce our model for constituent quarks and gluons restricted to a system with two flavors. Scale invariance is implemented in a linear σ model via the following Lagrangian:[1]

$$\begin{aligned}\mathcal{L} &= \bar{q}i\partial\!\!\!/ q + G_S\bar{q}(\sigma + i\vec{\tau}\cdot\vec{\pi})q + \frac{1}{2}(\partial_\mu\sigma\,\partial^\mu\sigma + \partial_\mu\pi\,\partial^\mu\pi) \\ &\quad + \frac{1}{2}\partial_\mu\chi\,\partial^\mu\chi - V_\sigma - V_\chi\,, \\ V_\sigma &= \frac{\lambda}{4}\left[(\sigma^2+\vec{\pi}^2) - \sigma_0^2\left(\frac{\chi}{\chi_0}\right)^2\right]^2 - \epsilon\left(\frac{\chi}{\chi_0}\right)^2\sigma\,, \\ V_\chi &= \frac{1}{4}B\left(\frac{\chi}{\chi_0}\right)^4\left[\ln\left(\frac{\chi}{\chi_0}\right)^4 - 1\right],\end{aligned} \tag{2.1}$$

where G_S is the scalar coupling constant and B is the bag constant. All other notations follow the standard linear σ model. We assume that the constituent gluons become massive due to the nonvanishing gluon condensate, $\langle\chi\rangle \neq 0$. This is achieved by introducing the Lagrangian for the constituent gluon field A_μ,

$$\mathcal{L}_A = -\frac{1}{4}A_{\mu\nu}A^{\mu\nu} + \frac{1}{2}G_A^2\left(\frac{\chi}{\chi_0}\right)^2 A_\mu A^\mu\,, \tag{2.2}$$

with the field strength tensor $A_{\mu\nu} = \partial_\mu A_\nu - \partial_\nu A_\mu$ and the coupling constant G_A to the dilaton field. The full Lagrangian is thus given by

$$\mathcal{L} \to \mathcal{L} + \mathcal{L}_A\,. \tag{2.3}$$

Here we assume that the quarks have no direct coupling to the gluons since the interaction between the quarks and gauge fields is embedded in G_S and G_A.

Applying the mean-field approximation, one finds the thermodynamic potential by performing the path integration

[1]There are some uncertainties on introducing χ in the explicit breaking term. See, e.g., Refs. [6,14]. This does not change our results.

over the quark and gluon fields:

$$\Omega = \Omega_q + \Omega_A + V_\sigma + V_\chi + \frac{1}{4}B\,,$$
$$\Omega_q = \gamma_q \int \frac{d^3p}{(2\pi)^3} T[\ln(1-n_q) + \ln(1-\bar{n}_q)]\,, \quad (2.4)$$
$$\Omega_A = -\gamma_A \int \frac{d^3p}{(2\pi)^3} T \ln(1+n_A)\,,$$

with the degeneracy factors for quarks $\gamma_q = 2N_f N_c = 12$ and for gluons $\gamma_A = 2(N_c^2 - 1) = 16$. A constant term is added so that $\Omega = 0$ at $T = \mu = 0$. The effective masses of the quasiparticles are defined by

$$M_q = G_S\sigma\,, \quad M_A = G_A\frac{\chi}{\chi_0}\,. \quad (2.5)$$

The thermal distribution functions are given by

$$n_q = \frac{1}{e^{(E_q-\mu)/T}+1}\,, \quad \bar{n}_q = \frac{1}{e^{(E_q+\mu)/T}+1}\,,$$
$$n_A = \frac{1}{e^{E_A/T}-1}\,, \quad (2.6)$$

with the quasiparticle energies $E_q = \sqrt{|\vec{p}|^2 + M_q^2}$ and $E_A = \sqrt{|\vec{p}|^2 + M_A^2}$.

The stationary condition, $\frac{\partial\Omega}{\partial\sigma} = \frac{\partial\Omega}{\partial\chi} = 0$, leads to the following coupled gap equations:

$$\gamma_q \int \frac{d^3p}{(2\pi)^3}\frac{M_q}{E_q} G_S(n_q + \bar{n}_q) + \lambda\sigma\left[\sigma^2 - \sigma_0^2\left(\frac{\chi}{\chi_0}\right)^2\right] - \epsilon\left(\frac{\chi}{\chi_0}\right)^2 = 0\,, \quad (2.7)$$

$$\gamma_A \int \frac{d^3p}{(2\pi)^3}\frac{M_A}{E_A} G_A n_A - \lambda\sigma_0^2\left[\sigma^2 - \sigma_0^2\left(\frac{\chi}{\chi_0}\right)^2\right]\frac{\chi}{\chi_0} - 2\epsilon\frac{\chi}{\chi_0}\sigma + B\left(\frac{\chi}{\chi_0}\right)^3 \ln\left(\frac{\chi}{\chi_0}\right)^4 = 0\,. \quad (2.8)$$

The mesonic parameters λ and ϵ are related with the σ and pion masses and the pion decay constant via

$$\lambda = \frac{m_\sigma^2 - m_\pi^2}{2f_\pi^2}\,, \quad \epsilon = m_\pi^2 f_\pi\,, \quad (2.9)$$

where the vacuum σ expectation value is $\sigma_0 = f_\pi$. In the following calculation we will use $m_\pi = 138$ MeV and $f_\pi = 93$ MeV and alter the vacuum σ mass m_σ in the range 0.6–1.2 GeV because of its uncertainty. The bag constant B and dimensionful parameter χ_0 are fixed by the vacuum energy density $\mathcal{E} = \frac{1}{4}B = 0.76$ GeV fm^{-3} [15] and the vacuum glueball mass $M_G = 1.7$ GeV [16] using the following definition:

$$M_G^2 = \frac{\partial^2 V_\chi}{\partial\chi^2} = \frac{4B}{\chi_0^2}\,. \quad (2.10)$$

The coupling constants G_S and G_A are determined by requiring that a nucleon is composed of three constituent quarks and a glueball of two constituent gluons, thus,

$$M_q(T=\mu=0) = \tfrac{1}{3}m_N = 300\,\text{MeV}\,,$$
$$M_A(T=\mu=0) = \tfrac{1}{2}M_G = 850\,\text{MeV}\,. \quad (2.11)$$

III. THERMODYNAMICS

The model introduced above describes the evolution of the two condensates, $\langle\sigma\rangle$ and $\langle\chi\rangle$, driven by temperature and chemical potential. Figure 1 shows the contours of the thermodynamic potential, taking the vacuum σ mass being $m_\sigma = 600$ MeV in the σ-χ plane at $\mu = 0$. As the temperature increases from zero, first the system experiences partial restoration of chiral symmetry at T_{chiral} indicated by the dropping σ, i.e., at which the chiral susceptibility becomes maximum, whereas another condensate χ remains almost a constant. Above T_{chiral}, the potential starts to exhibit a metastable state at $\sigma \sim \chi \sim 0$, and a first-order phase transition takes place at $T_{\chi=0}$ where the scale symmetry broken by nonvanishing χ is restored. Farther above this temperature, the system remains at the trivial ground state.

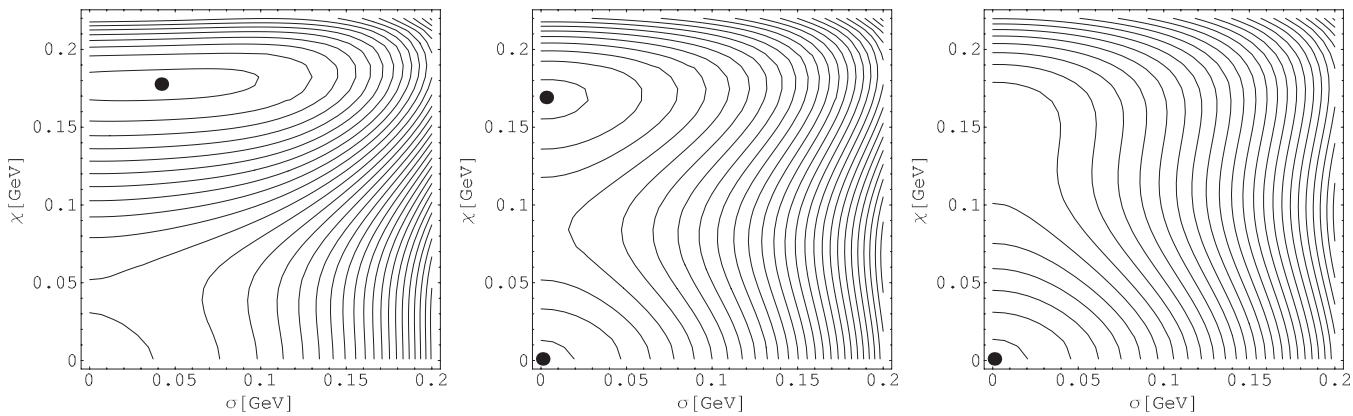

FIG. 1. Contour plots of the thermodynamic potential at finite T and $\mu = 0$: $T = 153$ MeV (chiral crossover), 251 MeV (first-order $\langle\chi\rangle \to 0$ transition), and 300 MeV from left to right. The black circle indicates the ground state. $m_\sigma = 600$ MeV at $T = 0$ was used. The pseudocritical temperature of chiral symmetry restoration was defined as the maximum temperature of the chiral susceptibility.

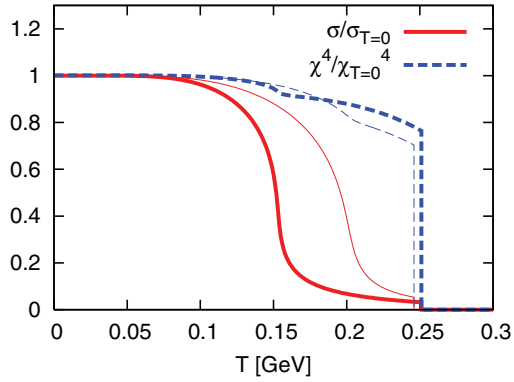

FIG. 2. (Color online) Normalized expectation values of σ and χ^4 fields at $\mu = 0$. The thick lines are calculated using $m_\sigma = 600$ MeV at $T = 0$ and the thin lines using $m_\sigma = 900$ MeV.

The thermal expectation values of σ and χ obtained from the gap equations in fact show a substantial reduction around the chiral crossover and a jump at the first-order transition as seen in Fig. 2. When the σ meson is very massive, $\lambda \to \infty$, one finds

$$\langle \sigma \rangle \simeq f_\pi \frac{\langle \chi \rangle}{\chi_0}, \tag{3.1}$$

corresponding to nonlinear realization of chiral Lagrangians, and the thermodynamics is governed by a single condensate. Near the chiral symmetry restoration point, the above relation between the two condensates is not expected since the σ meson cannot be integrated out. The condensate of the dilaton field has a weak sensitivity to temperature even above the chiral crossover and therefore it does not drive the disappearance of the chiral condensate. This feature, however, strongly depends on the σ-meson mass; and for a larger m_σ, the gluon condensate is more affected by the chiral phase transition, as we will discuss below.

In-medium masses of σ and χ fields are defined by

$$M_\sigma^2 = \left.\frac{\partial^2 \Omega}{\partial \sigma^2}\right|_{\sigma=\langle\sigma\rangle,\chi=\langle\chi\rangle}, \quad M_\chi^2 = \left.\frac{\partial^2 \Omega}{\partial \chi^2}\right|_{\sigma=\langle\sigma\rangle,\chi=\langle\chi\rangle}. \tag{3.2}$$

Their behavior as functions of temperature is given in Fig. 3. Increasing temperature toward $T_{\rm chiral}$, M_σ shows a strong sensitivity to the phase transition as observed in the standard linear σ models, whereas M_χ is rather modest. The two masses exhibit a jump when χ vanishes. Above this temperature, they follow a linear dependence of temperature, $M_{\sigma,\chi} \sim T$, as expected.

In Fig. 4 we show the energy density at $\mu = 0$ as a function of temperature. The standard linear σ model (LσM) almost follows the curves below $T_{\rm chiral}$, but strongly underestimates the Stefan-Boltzmann (SB) limit, which is a typical drawback of this model. Since the LσM Lagrangian does not contain gluons, bulk thermodynamics quantities are qualitatively in good agreement with the lattice results when they are normalized by the SB limit for massless quarks, whereas not when normalized by the SB limit for massless quarks and gluons. What we carried out in this paper is to improve the LσM by introducing missing gluons. As shown in the figure, the SB limit is now reproduced. A defect to be removed is

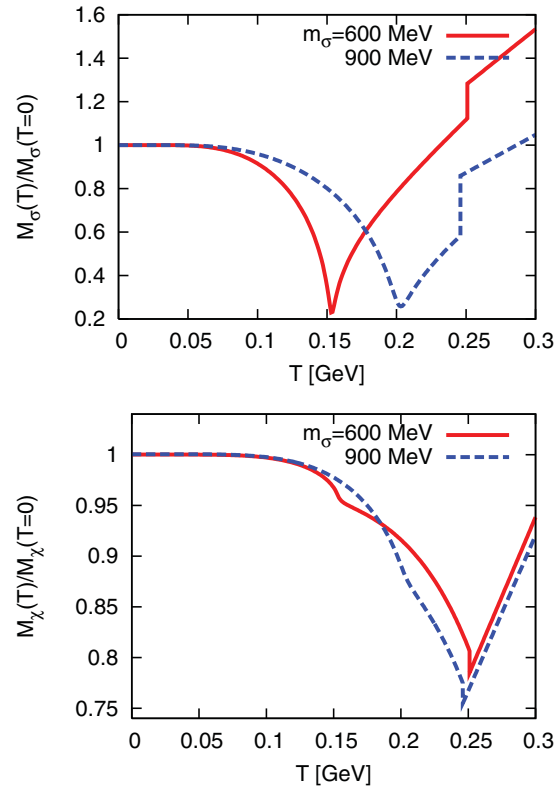

FIG. 3. (Color online) Thermal masses of σ (top) and χ (bottom) fields at $\mu = 0$.

the too strong first-order phase transition even at $\mu = 0$ which is absent in lattice QCD. Also, according to lattice QCD, the energy density should approach the SB limit from below. We remark that direct comparison must be carried out in a more realistic framework beyond the mean-field approximation. As shown in Refs. [10,18,19], including thermal and quantum fluctuations of meson fields will be particularly important around T_c.

The trace anomaly exists at any temperature which is the only dimension-full quantity which breaks scale invariance of the theory explicitly. In our model, at high temperature and $M_q \ll T$, the pressure and energy density at $\mu = 0$

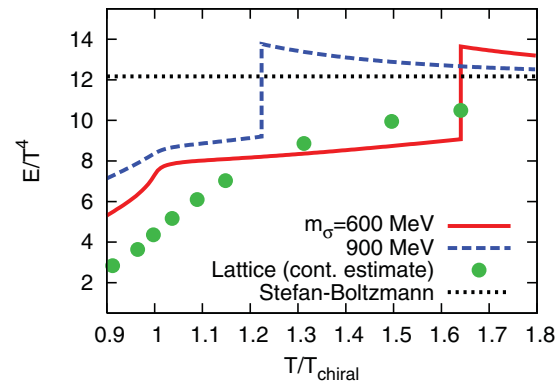

FIG. 4. (Color online) Scaled energy density at $\mu = 0$. The filled circles are the corresponding lattice data after continuum extrapolation taken from Ref. [17].

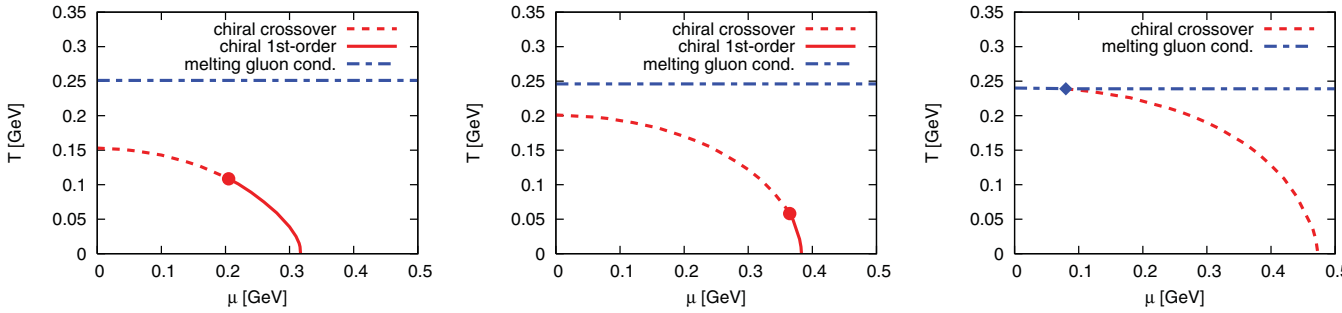

FIG. 5. (Color online) Phase diagram for different vacuum m_σ: $m_\sigma = 0.6$ GeV (left), 0.9 GeV (middle), and 1.2 GeV (right). The filled circle indicates the critical point, and the diamond the point where the first-order and crossover lines intersect.

are approximately expressed as

$$P = \gamma_q \frac{7\pi^2}{720} T^4 - \frac{\gamma_q}{48} M_q^2 T^2 - \frac{1}{4} B\,,$$
$$\mathcal{E} = \gamma_q \frac{21\pi^2}{720} T^4 - \frac{\gamma_q}{48} M_q^2 T^2 + \frac{1}{4} B\,. \tag{3.3}$$

Consequently, one finds the trace anomaly (interaction measure) as

$$\Delta(T) = \frac{\mathcal{E} - 3P}{T^4} = \frac{B}{T^4} + \frac{\gamma_q M_q^2}{24 T^2}\,. \tag{3.4}$$

Lattice calculations [17,20–22] show that Δ has a nonperturbative term, $\Delta \sim 1/T^2$ [23]. We see that this kind of contribution comes from the masses of quasiparticles. However, the numerical value associated with the effective quark mass in Eq. (3.4) is too small to explain this effect. Fluctuations beyond the mean-field approximation will also contribute to the interaction measure [10].

Turning on the quark chemical potential μ practically does not affect the temperature at which the gluon condensate vanishes, $T_{\chi=0}$, whereas the chiral transition boundary exhibits an elliptic shape and a critical point appears at an intermediate μ, shown in Fig. 5 (left). The boundary line of $T_{\chi=0}$ in general has a certain μ dependence via the gap equations. However, the σ expectation value above $T_{\rm chiral}$ is small and little affects $\langle\chi\rangle$. On the other hand, the chiral crossover line gets modified significantly depending on the m_σ chosen in vacuum. For larger m_σ the phase boundary is systematically shifted to higher T and μ. The critical point also moves toward lower T and eventually disappears from the phase diagram [24]. This is illustrated in Fig. 5 (middle and right). The thermodynamics at low temperature and high chemical potential is essentially the same as in the standard linear σ model.

Making a matching of the trace anomaly between the model and QCD would constrain a reliable range of m_σ. The divergence of the dilatation current is given by [7]

$$\partial_\mu J^\mu = -B\left(\frac{\langle\chi\rangle}{\chi_0}\right)^4 + \left(4 - T\frac{\partial}{\partial T} - \chi\frac{\partial}{\partial\chi}\right)\Omega_A|_{\chi=\langle\chi\rangle}\,. \tag{3.5}$$

The left side of the above equation is mostly saturated by the gluon condensate in QCD:

$$\partial_\mu J^\mu = -\left(\frac{11}{24}N_c - \frac{1}{12}N_f\right)\left\langle\frac{\alpha_s}{\pi}G^a_{\mu\nu}G^{\mu\nu}_a\right\rangle, \tag{3.6}$$

where a small contribution due to the explicit breaking of chiral symmetry is neglected. Lattice QCD calculations show that the thermal gluon condensate decreases toward the pseudocritical temperature of chiral symmetry restoration and drops down to a half of its vacuum value at $T_{\rm chiral}$, whereas it is quite stable at lower temperatures [12]. This is also a compatible feature with the QCD trace anomaly in terms of the soft and hard dilatons [25], i.e., the disappearance of the soft dilaton is associated with chiral symmetry restoration and yields the melting gluon condensate, or partial restoration of the scale symmetry breaking [26]. Equations (3.5) and (3.6) tend to match for a large $m_\sigma \sim 1$ GeV. With a small m_σ the gluon condensate does not show a significant drop at $T_{\rm chiral}$. Thus, a rather heavy σ-meson in the vacuum seems to be favored by QCD, and this is a conceivable scenario known from the vacuum phenomenology of the scalar mesons. It should be noted that the matching is somewhat incomplete: Eq. (3.5) exceeds Eq. (3.6) by ∼15%. This may indicate that a stronger interaction between the quark and gluon sectors should be introduced. Besides, updating the gluon condensate at finite temperature in lattice QCD is necessary.

IV. LIMIT OF INFINITELY HEAVY σ MESON

It is instructive to study the phase diagram in the $\lambda \to \infty$ limit where the σ meson becomes infinitely heavy. As discussed in the previous section, the two critical temperatures, $T_{\chi=0}$ and $T_{\rm chiral}$, get closer with increasing m_σ. With $m_\sigma \sim 1$ GeV they are almost on top of each other and larger m_σ yields an intersection of the first-order phase transition of scale symmetry and chiral crossover lines at finite μ. This intersection moves to higher μ and lower T for larger m_σ as shown in Fig. 6. The boundary line of scale symmetry restoration is less sensitive to μ when the chiral symmetry is restored. This is because the major μ dependence comes in via the σ expectation value $\langle\sigma\rangle$ which is well suppressed in restored phase. When m_σ reaches infinity, the intersection is kicked out and a single line of the first-order phase transition

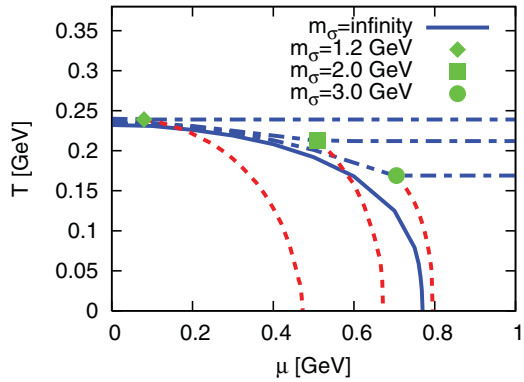

FIG. 6. (Color online) Phase diagram for different m_σ. The line notation is the same as in Fig. 5.

is left. The region where chiral symmetry is restored whereas $\langle\chi\rangle \neq 0$ is unfavored in this limit.

The parameters of effective Lagrangians can alter with T and μ since they are obtained by integrating higher frequency modes out and thus expected to carry information on the underlying QCD. Consequently, the phase diagram calculated with the parameters fixed using the vacuum quantities would be deformed, and the first-order phase transition could remain on the phase diagram at high μ in a cold system.

V. IMPLICATIONS FOR THE QCD PHASE DIAGRAM

The present toy model exhibits three regions characterized by the two condensates: (i) broken phase of chiral and scale symmetries, (ii) chirally restored but broken phase of the scale symmetry because of the nonvanishing $\langle\chi\rangle$, and (iii) chirally restored but explicitly broken phase of the scale symmetry by temperature. What does the thermodynamics of the model suggest concerning the QCD phase structure? The vanishing condensate of the dilaton field indicates a disappearance of the gluon composite at high temperature, and its dissociation may signal a transition of the system from the confined to deconfined phase. Thus, one identifies the temperature $T_{\chi=0}$ with a temperature at which gluons are released:

$$T_{\chi=0} \sim T^{(g)}_{\rm deconf}\,. \tag{5.1}$$

The model yields a chiral transition temperature that is below $T_{\chi=0}$ in a wide range of the parameters. In $N_f = 2$ QCD, this is compatible with the anomaly matching which is often used to constrain possible massless excitations in quantum field theories [27], and therefore the chirally restored phase with confinement is allowed. This suggests that the chiral symmetry restoration takes place either below or at the deconfinement temperature, i.e.,

$$T_{\rm chiral} \lesssim T^{(q)}_{\rm deconf}\,, \tag{5.2}$$

where at $T^{(q)}_{\rm deconf}$ the quarks are released whereas the gluons remain confined and it is not necessarily equal to $T^{(g)}_{\rm deconf}$. As we have seen in the previous section, a large m_σ can match with the QCD requirement at $\mu = 0$. This leads to the three distinct temperatures which may be close to each other

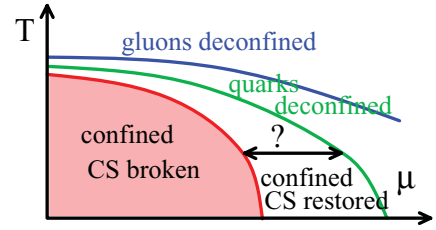

FIG. 7. (Color online) Sketch of the QCD phase diagram.

on the phase diagram. We note that this is consistent with the recent observation using a renormalization group analysis where the fixed point of four-fermion interactions associated with confinement plays an essential role [28]. At finite μ no reliable constraint from QCD is known. A suggestive phase diagram is given in Fig. 7.

VI. CONCLUSIONS AND REMARKS

In this paper we have studied thermodynamics and the phase structure of a QCD-like model whose degrees of freedom are constituent quarks and gluons. Both chiral and scale symmetries are implemented in the model by introducing mean fields representing $\bar{q}q$ and $G_{\mu\nu}G^{\mu\nu}$. These symmetries are dynamically broken at low temperature and density. The model thus mimics the features of QCD in the strong coupling region, i.e., the spontaneous breaking of chiral symmetry and trace anomaly. The results suggest that a system in deconfined phase develops gradually with increasing temperature and density toward weakly interacting quark-gluon matter composed of almost massless quarks and gluons.

The condensates of the σ and dilaton fields are dynamically linked via their gap equations. How strong they are correlated depends crucially on the σ-meson mass m_σ chosen in vacuum. We found that a large $m_\sigma \sim 1$ GeV is consistent with the lattice result regarding the thermal behavior of the gluon condensate. This further leads to the chiral phase transition which takes place almost simultaneously with the deconfinement transition at $\mu \sim 0$. At finite μ these two transitions are expected to be separated.

In the scalar sector of low-mass hadrons, scalar quarkonium, tetra-quark states [29], and glueballs are expected to be all mixed. How this can happen has been studied in certain simple models; see, e.g., Ref. [30] and references therein. An issue to be explored is how the presence of the tetra-quark modifies the phase structure presented in this work.

As an alternative approach one can use a parity doublet model assuming a certain assignment of chirality to nucleons with positive and negative parity [31,32]. As proposed in Refs. [33,34], the gluon condensate, more precisely the hard dilaton condensate, yields a chiral invariant mass of the nucleon, which stays nonvanishing above the chiral phase transition point. It is interesting to explore the thermodynamics of a parity doublet model [35] embedding dilatons, and this will be reported elsewhere.

The present model can also be applied to a nonequilibrium system, where the time evolution of the gluon condensate is described by the equation of motion for the dilaton. On the

other hand, in several models with Polyakov loops [23,36,37] it is unclear how the kinetic term of the Polyakov loop dynamically emerges, since the Polyakov loop by itself does not represent a field but rather a character of the SU(3) color group. It would be interesting to extend the work done in Ref. [38] along this line.

ACKNOWLEDGMENTS

This work has been partly supported by the Hessian LOEWE initiative through the Helmholtz International Center for FAIR (HIC for FAIR), and by Grants No. NS-7235.2010.2 and No. RFBR 09-02-91331 (Russia).

[1] J. C. Collins, A. Duncan, and S. D. Joglekar, Phys. Rev. D **16**, 438 (1977); N. K. Nielsen, Nucl. Phys. B **120**, 212 (1977).
[2] W. A. Bardeen, C. N. Leung, and S. T. Love, Phys. Rev. Lett. **56**, 1230 (1986).
[3] For recent reviews, see, e.g., R. S. Hayano and T. Hatsuda, Rev. Mod. Phys. **82**, 2949 (2010); R. Rapp, J. Wambach, and H. van Hees, arXiv:0901.3289; W.-G. Paeng and M. Rho, Mod. Phys. Lett. A **25**, 399 (2010); K. Fukushima and T. Hatsuda, Rep. Prog. Phys. **74**, 014001 (2011).
[4] J. Schechter, Phys. Rev. D **21**, 3393 (1980).
[5] B. A. Campbell, J. R. Ellis, and K. A. Olive, Nucl. Phys. B **345**, 57 (1990); Phys. Lett. B **235**, 325 (1990).
[6] G. E. Brown and M. Rho, Phys. Rev. Lett. **66**, 2720 (1991).
[7] K. Kusaka and W. Weise, Z. Phys. A **343**, 229 (1992); Nucl. Phys. A **580**, 383 (1994).
[8] I. Mishustin, J. Bondorf, and M. Rho, Nucl. Phys. A **555**, 215 (1993).
[9] A. Peshier, B. Kampfer, O. P. Pavlenko, and G. Soff, Phys. Rev. D **54**, 2399 (1996); P. Levai and U. W. Heinz, Phys. Rev. C **57**, 1879 (1998).
[10] G. W. Carter, O. Scavenius, I. N. Mishustin, and P. J. Ellis, Phys. Rev. C **61**, 045206 (2000).
[11] A. Dumitru, Y. Guo, Y. Hidaka, C. P. K. Altes, and R. D. Pisarski, Phys. Rev. D **83**, 034022 (2011); P. Castorina, D. E. Miller, and H. Satz, Eur. Phys. J. C **71**, 1673 (2011).
[12] D. E. Miller, Phys. Rep. **443**, 55 (2007).
[13] B. J. Schaefer, O. Bohr, and J. Wambach, Phys. Rev. D **65**, 105008 (2002).
[14] H. Gomm, P. Jain, R. Johnson, and J. Schechter, Phys. Rev. D **33**, 801 (1986).
[15] S. Narison, Nucl. Phys. Proc. Suppl. A **54**, 238 (1997).
[16] J. Sexton, A. Vaccarino, and D. Weingarten, Phys. Rev. Lett. **75**, 4563 (1995).
[17] S. Borsanyi *et al*. (Wuppertal-Budapest Collaboration), J. High Energy Phys. 09 (2010) 073.
[18] A. Mocsy, I. N. Mishustin, and P. J. Ellis, Phys. Rev. C **70**, 015204 (2004).
[19] J. I. Kapusta and E. S. Bowman, in *CPOD2009 Proceedings*, PoS(CPOD2009)018 (SISSA, Trieste, Italy, 2009).
[20] G. Boyd, J. Engels, F. Karsch, E. Laermann, C. Legeland, M. Lutgemeier, and B. Petersson, Nucl. Phys. B **469**, 419 (1996).
[21] G. Endrodi *et al*., J. High Energy Phys. 04 (2011) 001; S. Durr *et al*., *ibid*. 08 (2011) 148; Phys. Lett. B **701**, 265 (2011); S. Borsanyi *et al*., J. High Energy Phys. 11 (2010) 077.
[22] A. Bazavov *et al*., arXiv:1111.1710; M. Cheng *et al*., Phys. Rev. D **81**, 054504 (2010); **81**, 054510 (2010).
[23] B.-J. Schaefer, J. M. Pawlowski, and J. Wambach, Phys. Rev. D **76**, 074023 (2007).
[24] B.-J. Schaefer and M. Wagner, Phys. Rev. D **79**, 014018 (2009).
[25] V. A. Miransky and V. P. Gusynin, Prog. Theor. Phys. **81**, 426 (1989).
[26] H. K. Lee and M. Rho, Nucl. Phys. A **829**, 76 (2009).
[27] G. 't Hooft, in *Recent Developments in Gauge Theories*, edited by G. 't Hooft *et al*. (Plenum, New York, 1980).
[28] J. Braun and A. Janot, Phys. Rev. D **84**, 114022 (2011).
[29] R. L. Jaffe, Phys. Rev. D **15**, 267 (1977); **15**, 281 (1977).
[30] A. Heinz, S. Struber, F. Giacosa, and D. H. Rischke, Phys. Rev. D **79**, 037502 (2009).
[31] C. Detar and T. Kunihiro, Phys. Rev. D **39**, 2805 (1989).
[32] D. Jido, M. Oka, and A. Hosaka, Prog. Theor. Phys. **106**, 873 (2001).
[33] C. Sasaki, H. K. Lee, W. G. Paeng, and M. Rho, Phys. Rev. D **84**, 034011 (2011).
[34] W. G. Paeng, H. K. Lee, M. Rho and C. Sasaki, arXiv:1109.5431.
[35] T. Hatsuda and M. Prakash, Phys. Lett. B **224**, 11 (1989); D. Zschiesche, L. Tolos, J. Schaffner-Bielich, and R. D. Pisarski, Phys. Rev. C **75**, 055202 (2007); C. Sasaki and I. Mishustin, *ibid*. **82**, 035204 (2010).
[36] K. Fukushima, Phys. Lett. B **591**, 277 (2004); C. Ratti, M. A. Thaler, and W. Weise, Phys. Rev. D **73**, 014019 (2006).
[37] E. Megias, E. R. Arriola, and L. L. Salcedo, Phys. Rev. D **74**, 065005 (2006).
[38] M. Nahrgang, M. Bleicher, S. Leupold, and I. Mishustin, arXiv:1105.1962.